IEEE Access
Multidisciplinary | Rapid Review | Open Access Journal

SPECIAL SECTION ON MISSION CRITICAL SENSORS AND SENSOR NETWORKS (MC-SSN)

Received January 27, 2019, accepted February 10, 2019, date of publication March 25, 2019, date of current version April 5, 2019.

*Digital Object Identifier 10.1109/ACCESS.2019.2899242*

# An Implantable Antenna Design for an Intelligent Health Monitoring System Considering the Relative Permittivity and Conductivity of the Human Body

**YANG LI, LICHENG YANG, WENQING DUAN, AND XIAONAN ZHAO**
Tianjin Key Laboratory of Wireless Mobile Communications and Power Transmission, Tianjin Normal University, Tianjin 300387, China
College of Electronic and Communication Engineering, Tianjin Normal University, Tianjin 300387, China

Corresponding author: Yang Li (liyang_tongxin@163.com)

This work was supported in part by the Tianjin Higher Education Creative Team Funds Program, in part by the Tianjin Municipal Natural Science Foundation under Grant 18JCYBJC86400, and in part by the Doctor Fund of Tianjin Normal University under Grant 52XB1604.

**ABSTRACT** In this paper, an intelligent health monitoring system based on body-centric wireless communications is studied, and implantable antennas are investigated. To design antennas for an intelligent health monitoring system, the effects of the relative permittivity and conductivity of a human body equivalent liquid on an implantable antenna are investigated via electromagnetic analysis. Two types of capsule antennas, an isolated type capsule antenna, and a surface type capsule antenna, are investigated and compared. An inner-layer implantable capsule dipole antenna with the characteristics of both a large effective electrical length and a small transmission loss is proposed. The methodology of the designed capsule antenna that obtains a maximum received power at 500 MHz by changing the internal impedance is also presented.

**INDEX TERMS** Intelligent body healthcare management, implantable antenna, relative permittivity, conductivity, transmission characteristic.

## I. INTRODUCTION

Both antenna technology and communication technology have gained popularity in applications related to intelligent body healthcare monitoring systems. A sensor or sensor network can be applied in intelligent health monitoring systems, and there have already been many previous studies that have focused on sensor networks [1]–[5]. An intelligent health monitoring system is based on body-centric wireless communications (BCWCs) [6]. The intelligent health monitoring system uses a wireless transceiver to obtain medical images in vivo [7]. Generally, the capsule has a maximum length of approximately 26 mm and a maximum diameter of approximately 10 mm, and it is assumed that the efficiency of the capsule antenna is extremely low due to its physical size [7]. Furthermore, the absorption of electromagnetic waves by the internal organs is quite large and the propagation loss through the human body is quite large.

The associate editor coordinating the review of this manuscript and approving it for publication was Qilian Liang.

In previous studies, several types of antennas were proposed for implantable applications. Approaches for making use of the inside space of the capsule were presented in [8]–[11], an antenna that was placed conformal with the inner wall of the capsule was developed in [9], and a wideband spiral antenna was proposed in [10]. However, all these antennas were not in direct contact with the human body medium. The approach of making use of the surface of a capsule was first presented in [11], where a loop antenna was fabricated on the outer wall of the capsule, which was in contact with the human body medium. However, a comparison of the antenna characteristics among these scenarios has not been sufficiently performed.

S. Gabriel et al. found that a homogenous material with a relative permittivity and conductivity similar to muscle could be used as a human body phantom material [12], [13]. Sato *et al.* [14] at Tohoku University suggested that it is important to obtain the correct simulation method and the correct experimental method as the first step in developing implantable antennas. The model in [15] is used to validate our simulation method, in which a cubic box filled

with deionized water and a dipole were used. The measurement results of the dipole antenna in deionized water were compared with the numerical analysis results. The results of finite-difference time-domain (FDTD) simulation and the results of the measurement are shown to have good agreement [14], [16], and the correct simulation method was obtained. Moreover, a kind of capsule antenna, namely, the dipole antenna, placed at the interface of the capsule, was also proposed, which is easy to match at 1 GHz [16].

In this paper, two types of previously proposed capsule antennas, namely, the isolated type capsule antenna and the surface type capsule antenna, are investigated and compared. The methodology of the design implantable capsule antenna considering the relative permittivity and conductivity are discussed. Finally, an inner-layer implantable capsule dipole antenna with the characteristics of both a good performance of impedance matching characteristics and a good performance of transmission characteristics is proposed by the FDTD analysis. The guidelines for designing capsule antennas by using the transmission factor and received power are then proposed.

This manuscript is organized as follows. A numerical human body phantom and simulation model is shown in Section 2. The geometries of the two kinds of previously proposed capsule antennas and the transmission factor are introduced in Section 3. In Section 4, the effects of the relative permittivity and conductivity on the capsule antenna are investigated. The proposed inner-layer capsule dipole antenna (ICDA) is proposed in Section 5. Finally, the results and observations are summarized in Section 6.

## II. NUMERICAL HUMAN BODY PHANTOM

In this study, a commercial human torso-shaped phantom named ''Torso'', developed by SPEAG Co. Ltd., is used as the container of the human body material in the numerical analysis, as shown in Figure 1. The shell of phantom is made of fiberglass ($\varepsilon_r = 3.5$) and the thickness is approximately 2 mm. The human torso-shaped phantom is filled with the human body equivalent liquid, which is a kind of human body material. The tissue simulating liquids is also developed by SPEAG Co. Ltd., and in this study, it can be abbreviated as ''TSL''. Figure 2 shows the relative permittivity and conductivity of the TSL. In the frequency range of 200 MHz to 2 GHz, there is no particularly difference between the value of the TSL and the measured data of human body tissues provided by Gabriel [12], [13]. An internal capsule antenna is placed inside the torso-shaped phantom at the position indicated as Port 1 ($x_1$, $y_1$, $z_1$), and an external receiving antenna is placed at Port 2 ($x_2$, $y_2$, $z_2$). The distance between two antennas is set to $D = 74$ mm.

## III. CAPSULE ANTENNA AND TRANSMISSION FACTOR

### A. CAPSULE ANTENNA

The dimensions of the cuboid capsules are 30 mm in length and 10 mm in width. The relative permittivity of the capsule is set as the air ($\varepsilon_r = 1$).

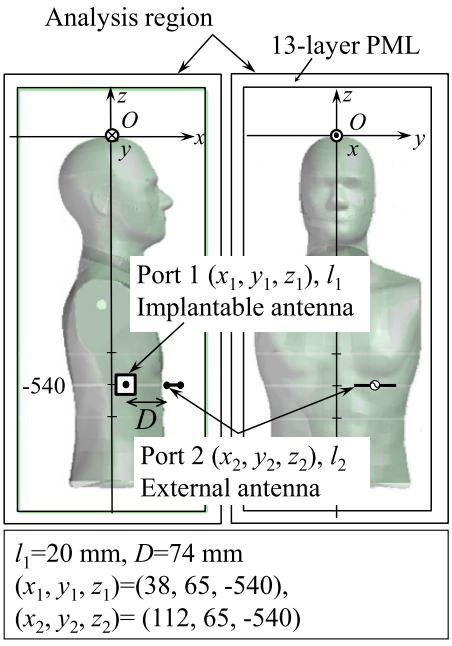


**FIGURE 1.** Analysis model: Torso-shaped human body phantom.

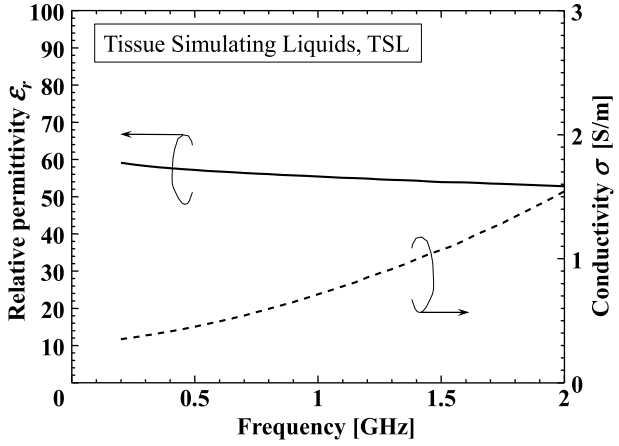


**FIGURE 2.** Relative permittivity and conductivity of the TSL.

The traditional capsule antenna type is an antenna set inside the capsule [9], [10]. In [11], a new type of capsule antenna was used: the antenna was set on the outer wall of the capsule to obtain a good impedance matching performance.

To investigate these two kinds of capsule antennas, the geometries of the two kinds capsule dipole antennas were proposed [15], as shown in Figure 3. The characteristics of the two types of capsule dipole antennas are shown in Figure 3. In case (a), the dipole antenna is placed inside the capsule with a distance of $d = 4$ mm to the center axis, and the antenna is isolated from the human body liquids so it can be called the ''isolated type capsule antenna'', while in case (b), the dipole antenna is placed on the surface of the capsule with a distance of $d = 5$ mm to the center axis, this means the

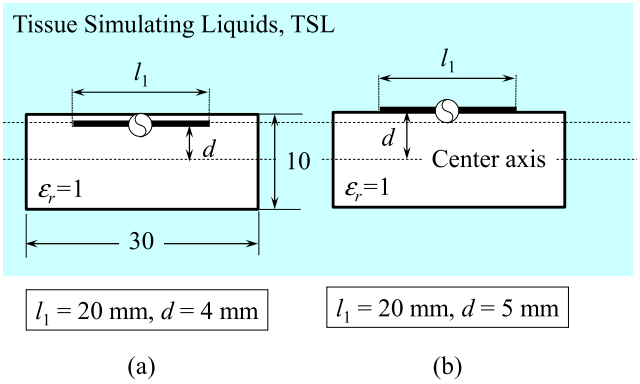


**FIGURE 3.** Geometries of the capsule antennas performed in [23]. (a) Isolated type capsule antenna. (b) Surface type capsule antenna.

antenna's surface touches to the human body liquids so it can be called the "surface type capsule antenna".

In the FDTD analysis, the cuboid shaped capsule was used. The number of cells was $202 \times 304 \times 462$. A Gaussian differential pulse was used as an excitation. A 13-layer perfectly matched layer (PML) was used as an absorbing boundary condition.

Figure 4 shows the frequency characteristics of the input impedance of the isolated type and the surface type capsule antenna. In the case of the isolated type capsule antenna, the dipole antenna with a length of 20 mm is an electric small antenna (compared to the wavelength) in the frequency range of 200 MHz to 2 GHz. The resistance is quite small ($R_{\text{in}} < 20\ \Omega$), while the reactance is negative ($X_{\text{in}} < 0$, capacitive). In the frequency range of 200 MHz to 2 GHz, the physical length of the dipole $l_1 < 0.15\lambda_0$ ($\lambda_0$: wavelength at 2 GHz) results in an electrically small antenna. In the case of the surface type capsule antenna, the resistance becomes large compared to the isolated type capsule antenna. It is also observed that the reactance is $X = 0$ at 1.2 GHz and 2 GHz. The wavelength in dielectric liquid therefore becomes small. Assuming an effective dielectric permittivity of

$$\varepsilon_g = \frac{\varepsilon_r + 1}{2} \tag{1}$$

when the dipole is implemented on the surface of the capsule, the effective wavelength $\lambda_g$ at 1.2 GHz becomes 50 mm when $\varepsilon_r = 49$, which is close to the twice the length of dipole $l_1 = 20$ mm. The resonance $X = 0$ at 1.2 GHz. The antenna conductor is implemented on the surface of the capsule and the effective wavelength is given by

$$\lambda_g \approx \frac{\lambda_0}{\sqrt{\varepsilon_g}} \tag{2}$$

where $\varepsilon_g$ is the effective dielectric permittivity approximated as in equation (1). The effective wavelength $\lambda_g = 47$ mm at 1.2 GHz when $\varepsilon_r = 55.4$ and $l_1 = 0.43\lambda_g$ is obtained. This means that the surface type capsule antenna is the half-wavelength dipole antenna at 1.2 GHz.

Figure 5(a) shows the reflection coefficient |S11| of the capsule dipole antennas in the cases of the isolated type and

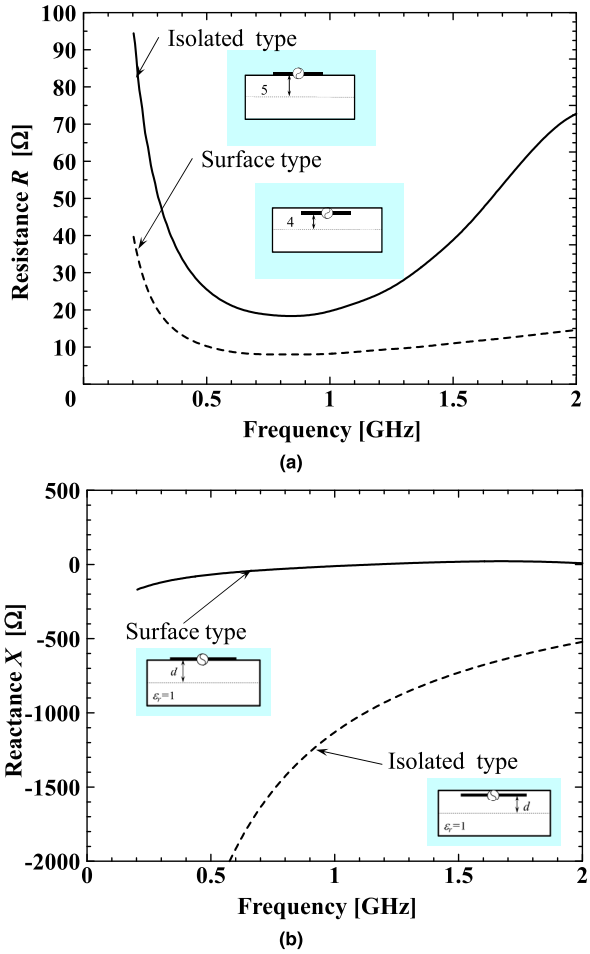


**FIGURE 4.** Impedance of the capsule antennas. (a) Resistance $R$. (b) Reactance $X$.

surface type capsule antennas. It is determined that in the case of the isolated type capsule antenna, |S11| is very large (approximately 0 dB) in the frequency range of 200 MHz to 2 GHz. However, in the case of the surface type capsule antenna, |S11| is relatively small in the frequency range of 200 MHz to 2 GHz. Figure 5(b) shows the transmission coefficient |S21| (matching to 50 Ω) from the capsule antenna through the torso-shaped phantom to the external antenna. In the case of the surface type capsule antenna, a high value of $|S21| = -28.9$ dB at 1 GHz is obtained. On the other hand, the maximum value in the case of the isolated type capsule antenna is −57.4 dB, and the value is small compared to the case of the surface type capsule antenna. These results show that a large value of the |S21| is obtained when the dipole antenna is implemented on the surface of the capsule, and it is considered that the electric length increases with the presence of the liquid. The half-wavelength resonant frequency of the receiving antenna at Port 2 is 1 GHz; the local maximum of |S21| in the frequency domain can be changed to other frequencies by changing the operating frequency of the receiving antenna. Additionally, it is observed that the transmission coefficients are almost the same for the case of without a capsule [19], [20] and the case of the antenna

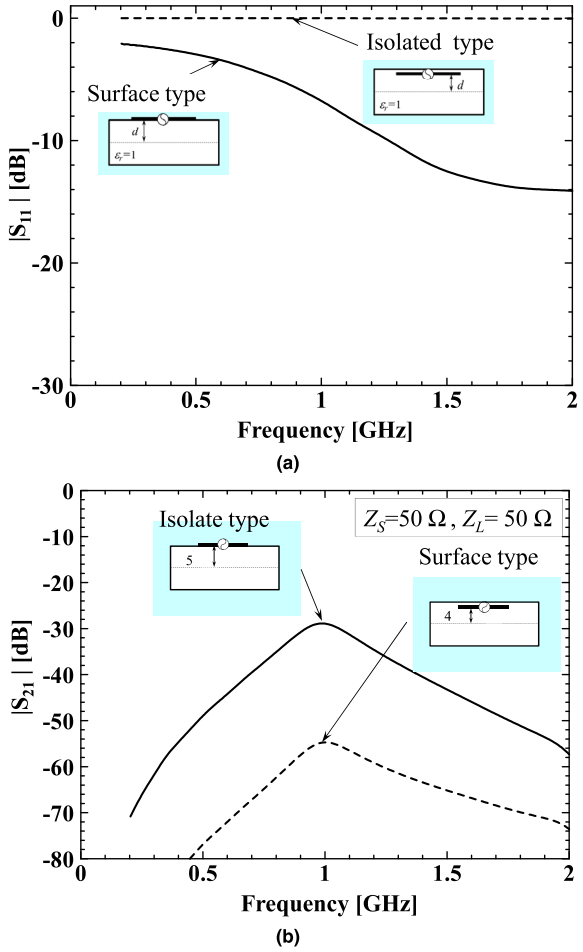


**FIGURE 5.** *S*-parameters of the capsule antennas. (a) Reflection coefficients. (b) Transmission coefficients.

on the surface of the capsule. It is considered that a dipole antenna implemented on the surface of the capsule has almost the same transmission characteristics as the case of a dipole antenna immersed in the TSL without a capsule.

### B. TRANSMISSION FACTOR

To compare the propagation loss between the different types of capsule antennas without considering the effect of antenna mismatching, the transmission factor $\tau$ [17], [18] could be used which is the relative maximum received power under the complex conjugate matching condition. The implantable antenna is connected to a source with an internal impedance of $Z_S$, while the external antenna is loaded with an internal impedance of $Z_L$. $P_L$ is the power delivered to the load $Z_L$, $P_{in}$ is the input power, $P_{inc}$ is the incident power, $\Gamma_S$ and $\Gamma_L$ are the reflection coefficients looking toward the source $Z_S$ and the load $Z_L$, respectively, and $\Gamma_{in}$ and $\Gamma_{out}$ are the reflection coefficients looking toward Port 1 and Port 2. The transmission factor is defined by [17] and [18]

$$\tau = \frac{P_L}{P_{inc}}\bigg|_{Z_S=Z_{in}^*, Z_L=Z_{out}^*} = \frac{P_L}{P_{in}} = \frac{1}{1-|\Gamma_S|^2}\,|S_{21}|^2\,\frac{1-|\Gamma_L|^2}{|1-S_{22}\Gamma_L|^2} \tag{3}$$

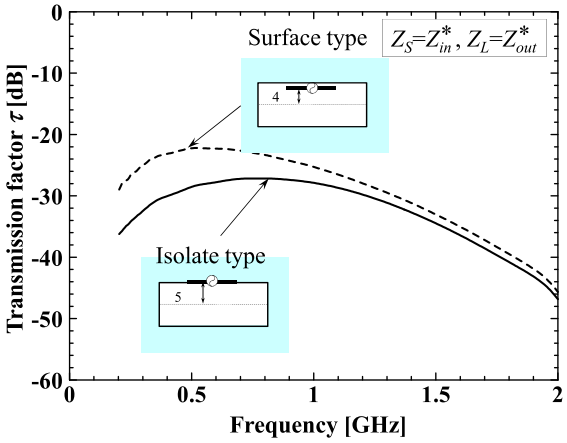


**FIGURE 6.** Transmission factors of the capsule antennas.

The optimal $Z_{S,opt}$ and $Z_{L,opt}$ are obtained by

$$Z_{S,opt} = Z_0\frac{1+\Gamma_S}{1-\Gamma_S}, \quad Z_{L,opt} = Z_0\frac{1+\Gamma_L}{1-\Gamma_L}. \tag{4}$$

Figure 6 shows the transmission factor from the capsule antenna through the torso-shaped phantom to the external antenna [21], [22]. The results in the case of the external dipole $l_2 = 140$ mm and in the case of the external dipole $l_2 = 280$ mm are the same. It is determined that there is a local maximum in the frequency domain. Because the conductivity loss becomes large when the dipole antenna is in contact with the liquid, the value of $\tau$ in the case of a surface type capsule antenna is smaller than that in the case of an isolated type capsule antenna. In the case of an isolated type capsule antenna, under the conditions $Z_S = 3.02 + j2467.22\ \Omega$ and $Z_L = 18.62 + j467.14\ \Omega$, a large value of $\tau = -20.0$ dB is obtained at 500 MHz. Briefly summarized, for the surface type capsule antenna, the value of transmission factor is large, but the impedance matching performance is not good, so additional matching circuits are necessary. For the isolated type capsule antenna, the impedance matching performance is good while the value of transmission factor is small. The relative permittivity of the material surrounding the antenna affects the impedance matching performance, and the conductivity of the material surrounding the antenna affects the transmission factor.

Figure 7 shows the received powers from the capsule antennas to the external dipole antenna through the human torso-shaped phantom. Local maxima of the transmission factor $\tau$ are observed for each case of the isolated type capsule antenna and the surface type capsule antenna. The reason why there is a local maximum is because there is a lower radiation efficiency in the low frequency range and higher conductivities in the high frequency range. The maximum values of $\tau = -26.9$ dB at 495 MHz and $\tau = -31.3$ dB at 500 MHz are obtained for the isolated type capsule antenna and the surface type capsule antenna, respectively. Under the condition of $Z_S = Z_{S,opt}$ and $Z_L = Z_{L,opt}$ at 500 MHz,

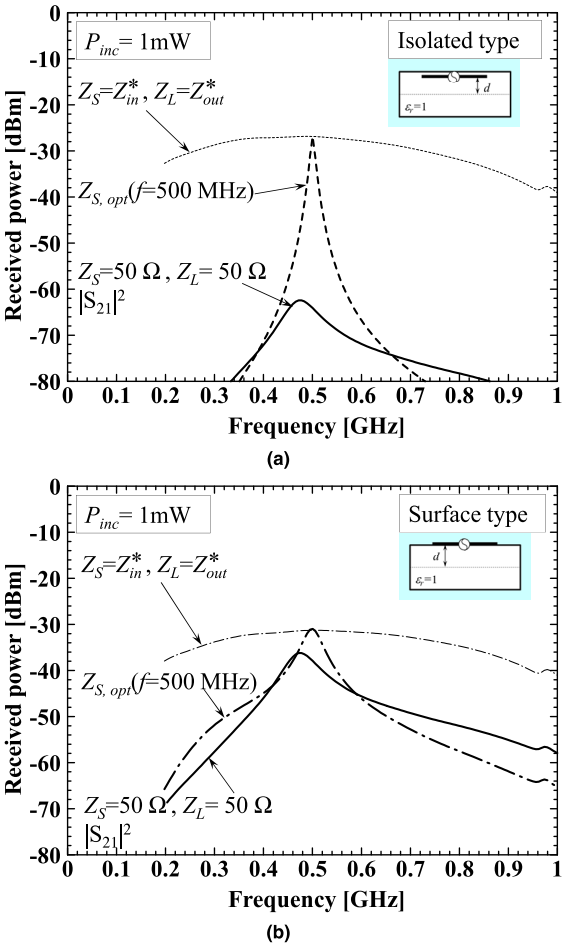


**FIGURE 7.** Received powers of the capsule antennas. (a) Isolated type capsule antenna. (b) Surface type capsule antenna.

the received power of −26.9 dBm and −31.3 dBm are obtained and a 3 dB-bandwidth of 7.6 MHz and 37 MHz are obtained for the isolated type in Figure 7(a) and for the surface type in Figure 7(b), respectively. Briefly summarizing the above results, the isolated type capsule antennas are electrical small antennas with poor performance on impedance matching; the surface type capsule antenna is an approximately half-wavelength antenna with a good performance on impedance matching to 50 Ω.

## IV. EFFECTS OF RELATIVE PERMITTIVITY AND CONDUCTIVITY ON THE CAPSULE ANTENNA

To study the effects of the relative permittivity and conductivity on the capsule antenna, it is necessary to use a frequency-independent material. Figure 8 shows the geometry of the capsule antenna filled with frequency-independent material. The dipole antenna is placed in the middle of the capsule, and there is a change in the relative permittivity and conductivity of the material surrounding the antenna. Three settles of materials are considered, (a) maintaining $\sigma = 0.6$ S/m, and changing $\varepsilon_r = 10$, $\varepsilon_r = 50$, and $\varepsilon_r = 80$ to observe the effect of the relative permittivity; (b) maintaining $\sigma = 0$ S/m, and changing $\varepsilon_r = 10$, $\varepsilon_r = 50$, and $\varepsilon_r = 80$ to observe the effect

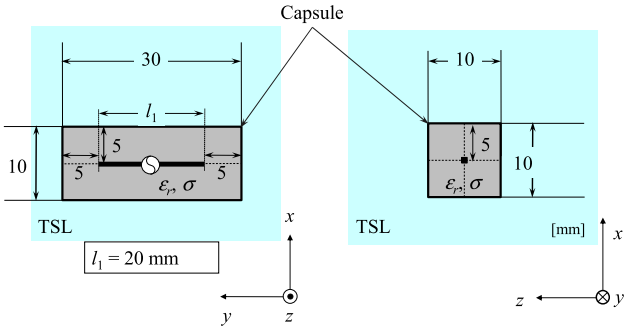


**FIGURE 8.** Geometries of the capsule antenna filled with material.

of the relative permittivity; and (c) maintaining $\varepsilon_r = 50$, and changing $\sigma = 0.1$ S/m, 0.6 S/m, and 2.0 S/m to observe the effect of the conductivity.

Figure 9(a) shows the results of maintaining $\sigma = 0.6$ S/m and changing the relative permittivity as $\varepsilon_r = 10$, $\varepsilon_r = 50$, and $\varepsilon_r = 80$. Under the condition of $Z_S = Z_{S,opt}$ and $Z_L = Z_{L,opt}$ at 500 MHz, received powers of −38.8 dBm, −31.3 dBm and −28.0 dBm are obtained in the cases of $\varepsilon_r = 10$, 50 and 80, respectively. In the case of $\varepsilon_r = 80$, the received power is the largest. The relative permittivity increase causes the effective electrical length of the antenna to increase, which causes the received power to increase. The 3 dB-bandwidth is 23 MHz for all these cases.

Figure 9(b) shows the results of maintaining $\sigma = 0$ S/m and changing the relative permittivity as $\varepsilon_r = 10$, $\varepsilon_r = 50$, and $\varepsilon_r = 80$. Under the condition of $Z_S = Z_{S,opt}$ and $Z_L = Z_{L,opt}$ at 500 MHz, received powers are almost same, approximately −22.3 dBm, larger than that under the condition of $\sigma = 0.6$ S/m in Figure 9(a). It is considered that the conductivity has a negative effect on the maximum received power.

Figure 9(c) shows the results of maintaining $\varepsilon_r = 50$ and changing the conductivity as $\sigma = 0.1$ S/m, $\sigma = 0.6$ S/m, and $\sigma = 2$ S/m. In the case of $\sigma = 0.1$ S/m, the received power is highest. Under the condition of $Z_S = Z_{S,opt}$ and $Z_L = Z_{L,opt}$ at 500 MHz, received powers of −25.7 dBm, −31.3 dBm and −33.2 dBm are obtained for the cases of $\sigma = 0.1$ S/m, 0.6 S/m, and 2.0 S/m, respectively. The small conductivity causes a small conductivity loss, which causes the received power to increase. The 3 dB-bandwidth is approximately 23 MHz for all these cases.

## V. INNER-LAYER CAPSULE DIPOLE ANTENNA (ICDA)

Based on the previous geometry of the capsule antenna and previous relationship between the relative permittivity and conductivity, an inner-layer capsule dipole antenna (ICDA) was proposed by Tohoku University in [23]. Figure 10(a) shows the geometry of the inner-layer capsule dipole antenna. An inner-layer with a thickness of 2 mm is made inside the capsule. The antenna conductor is placed in the inner-layer of deionized water provided inside the capsule with a thickness of 2 mm. Figure 10(b) shows the relative permittivity and conductivity of the deionized water [14]. Deionized water

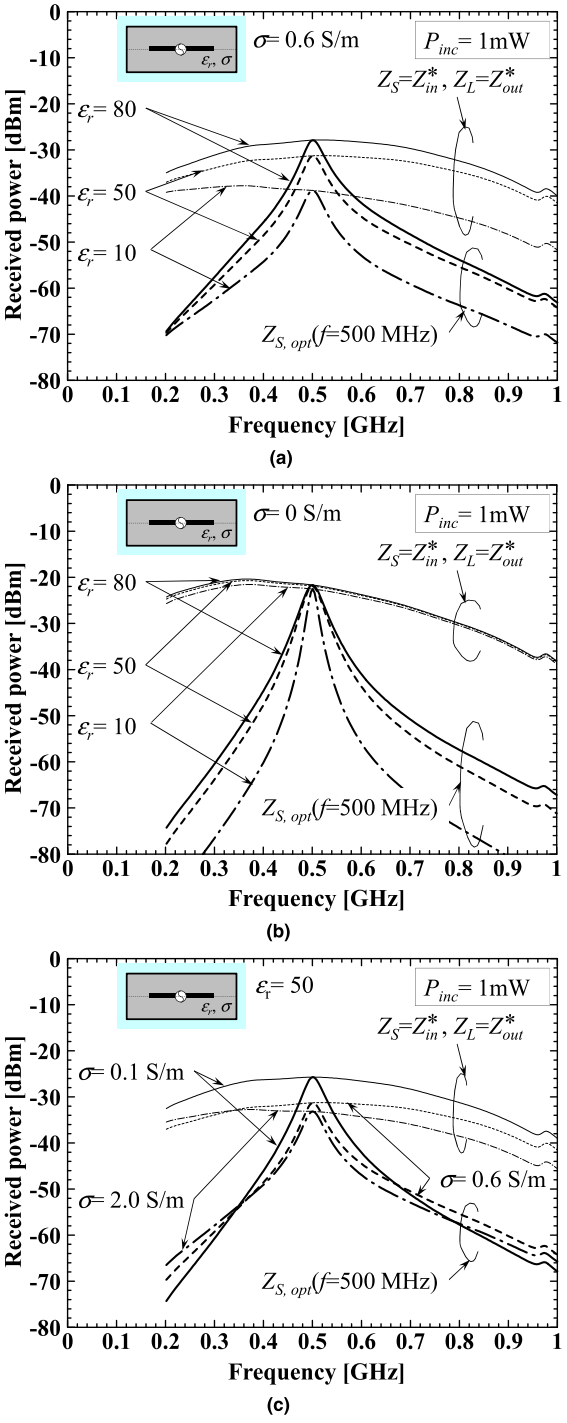


**FIGURE 9.** Received power of the capsule antenna filled with frequency-independent material. (a) $\sigma$ = 0.6 S/m, (b) $\sigma$ = 0 S/m, (c) $\varepsilon_r$ = 50.

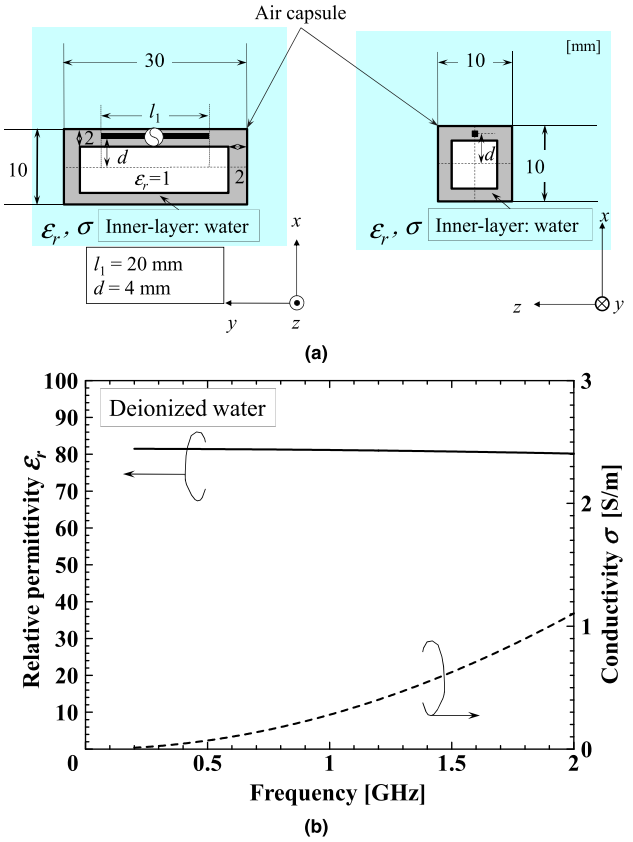


**FIGURE 10.** Geometries of the proposed ICDA. (a) Geometry. (b) Relative permittivity and conductivity of deionized water.

was used to fill the inner-layer because its relative permittivity is large and its conductivity is small compared to the TSL. The relative permittivity of the TSL is smaller and the conductivity is larger than that of deionized water.

Figure 11 shows the transmission coefficient |S21| (matching to 50 Ω) from the proposed ICDA through the torso-shaped phantom to the external antenna. Figure 11(a) shows the results when the external antenna has a length of $l_2$ = 140 mm (operating frequency: 1 GHz): in the case of ICDA, a relatively high value of |S21| = −26.6 dB was obtained, while in the case of the isolated type capsule antenna, the maximum value was −53.8 dB at 980 MHz. Figure 11(b) shows the results when the external antenna has a length of $l_2$ = 280 mm (operating frequency: 500 MHz): in the case of the ICDA, a relatively high value of |S21| = −30.4 dB was obtained, while in the case of separated type antenna, the maximum value was −61.6 dB at 500 MHz. Compared to the isolated type capsule antenna, the impedance matching condition improves and a large value of |S21| is obtained.

Figure 12 shows the results of the transmission factor $\tau$ from the proposed ICDA through the torso-shaped phantom to the external antenna. Compared to the isolated type capsule antenna and surface type capsule antenna, the transmission factor $\tau$ of the ICDA has the highest value, especially approximately 500 MHz. The negative effect of the high conductivity TSL on the transmission characteristics has been eliminated.

Figure 13 shows the results of the received power from the implantable capsule antenna to the external antenna. Figure 13(a) shows the comparison between the isolated type and the proposed ICDA under the different impedance matching conditions. In the case of the isolated type capsule antenna, under the condition of $Z_S$ = 10.2 + *j*2306 Ω and

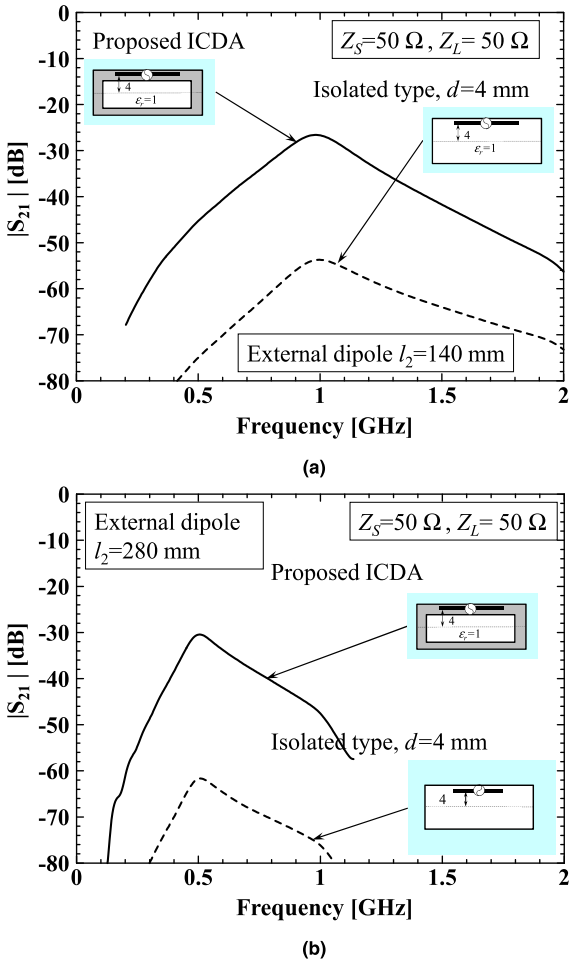


**FIGURE 11.** Transmission coefficients from the capsule antenna to the external antennas. (a) External dipole $l_2$ = 140 mm. (b) External dipole $l_2$ = 280 mm.

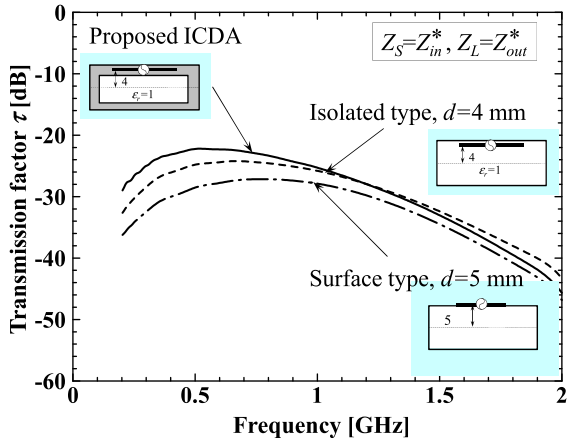


**FIGURE 12.** Transmission factors of the three types implantable capsule antennas.

$Z_L = 18.9 + j480\ \Omega$, a large received power of −24.7 dBm is obtained at 500 MHz, and the 3 dB-bandwidth is 28 MHz. In the case of the proposed ICDA, under the condition of $Z_S = 50\ \Omega$ and $Z_L = 50\ \Omega$, an acceptable power of −30.4 dBm is

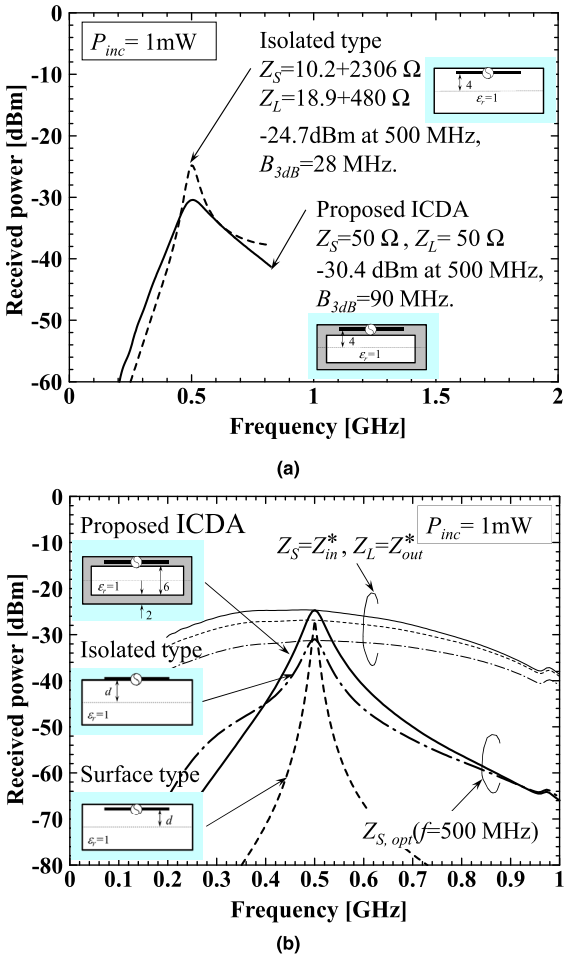


**FIGURE 13.** Received power of the proposed ICDA. (a) Comparison between the isolated type and the proposed ICDA under the different impedance matching conditions. (b) Comparison among the three types implantable capsule antennas under the same impedance matching conditions [23].

obtained at 500 MHz, and a wide 3 dB-bandwidth, approximately 90 MHz is obtained. Above all, the proposed ICDA has an acceptable impedance matching performance to 50 Ω in the frequency range of 500 MHz to 1 GHz. Figure 13(b) shows the comparison among the three types implantable capsule antennas [23]. It is determined that under the condition of $Z_S = Z_{S,opt}$ and $Z_L = Z_{L,opt}$ at 500 MHz, a received power of −24.7 dBm is obtained. The 3 dB-bandwidth is approximately 39 MHz. Compared to the isolated type capsule antenna and the surface type capsule antenna, the proposed inner-layer capsule dipole antenna is almost a half-wavelength antenna, so it can easily match the input impedance to 50 Ω. The received power is relatively large which will be caused by the lower conductive current around the feeding point compared with the surface type capsule antenna that is touching the lossy TSL.

## VI. CONCLUSION

In this study, an implantable capsule antenna design considering the relative permittivity and conductivity was investigated. The electromagnetic wave propagation characteristics

from different types of capsule antennas to the exterior were performed and compared in the frequency range of 200 MHz to 2 GHz. The results were obtained using the electromagnetic simulation software SEMCAD.

In the case of the isolated type capsule antenna, the antenna is separated from the human body liquid, so the conductivity loss is small, while the impedance matching is bad in the frequency range of 200 MHz to 2 GHz. In the case of the surface type capsule antenna, the antenna is in contact with the human body liquid, so the impedance matching is good in the frequency range of 1 GHz to 2 GHz, while the conductivity loss is large. In practical applications, if the size of the implantable capsule is strictly limited, the antenna can be implemented on the surface of the capsule to save space, and matching circuits are not required. Otherwise, if a high received power is strictly required, an antenna implemented inside the capsule with matching circuits is preferred.

An inner-layer capsule dipole antenna (ICDA) was proposed and investigated. It has both a good impedance matching performance of 50 Ω and a small conductive loss in the frequency range of 500 MHz to 1 GHz. It was determined that the inner-layer of deionized water provided in the air capsule contributed to enlarging the effective electrical size of the dipole antenna and contributed to decreasing the conductive current loss at the feeding point, resulting in a high received power through the human body phantom. Although conical models of the antennas were used in the numerical analysis models, these results and observations are general and fundamental. They can provide theoretical insight on how to design capsule antennas by using transmission factor. In practice, the antenna geometry can be designed to be very complex and the results in this study are still applicable.

## ACKNOWLEDGMENTS

The authors would like to thank Professor Qiang Chen at Tohoku University for allowing us to use the computer with the electromagnetic software installed in his lab. The authors would like to thank Professor Qiang Chen and Professor Hiroyasu Sato at Tohoku University for their constructive suggestions. The authors would also like to thank everyone at Chen Laboratory, Tohoku University, for their help with this article.

## REFERENCES

[1] Q. Liang, X. Cheng, S. C. Huang, and D. Chen, "Opportunistic sensing in wireless sensor networks: Theory and application," *IEEE Trans. Comput.*, vol. 63, no. 8, pp. 2002–2010, Aug. 2014.

[2] Q. Liang, "Situation understanding based on heterogeneous sensor networks and human-inspired favor weak fuzzy logic system," *IEEE Syst. J.*, vol. 5, no. 2, pp. 156–163, Jun. 2011.

[3] Q. Liang, X. Chen, and S. W. Samn, "NEW: Network-enabled electronic warfare for target recognition," *IEEE Trans. Aerosp. Electron. Syst.*, vol. 46, no. 2, pp. 558–568, Apr. 2010.

[4] Q. Liang and X. Cheng, "KUPS: Knowledge-based ubiquitous and persistent sensor networks for threat assessment," *IEEE Trans. Aerosp. Electron. Syst.*, vol. 44, no. 3, pp. 1060–1069, Jul. 2008.

[5] Q. Liang, B. Zhang, C. Zhao, and Y. Pi, "TDoA for passive localization: Underwater versus terrestrial environment," *IEEE Trans. Parallel Distrib. Syst.*, vol. 24, no. 10, pp. 2100–2108, Oct. 2013.

[6] P. S. Hall and Y. Hao, *Antennas and Propagation for Body-Centric Wireless Communications*, 2nd ed. London, U.K.: Artech House, 2012, pp. 586–589.

[7] G. Iddan, G. Meron, A. Glukhovsky, and P. Swain, "Wireless capsule endoscopy," *Nature*, vol. 405, p. 417, May 2000.

[8] L. C. Chirwa, P. A. Hammond, S. Roy, and D. R. S. Cumming, "Electromagnetic radiation from ingested sources in the human intestine between 150 MHz and 1.2 GHz," *IEEE Trans. Biomed. Eng.*, vol. 50, no. 4, pp. 484–492, Apr. 2003.

[9] P. M. Izdebski, H. Rajagopalan, and Y. Rahmat-Samii, "Conformal ingestible capsule antenna: A novel chandelier meandered design," *IEEE Trans. Antennas Propag.*, vol. 57, no. 4, pp. 900–909, Apr. 2009.

[10] S. H. Lee *et al.*, "A wideband spiral antenna for ingestible capsule endoscope systems: Experimental results in a human phantom and a pig," *IEEE Trans. Biomed. Eng.*, vol. 58, no. 6, pp. 1734–1741, Jun. 2011.

[11] S. Yun, K. Kim, and S. Nam, "Outer-wall loop antenna for ultrawideband capsule endoscope system," *IEEE Antennas Wireless Propag. Lett.*, vol. 9, pp. 1135–1138, Dec. 2010.

[12] S. Gabriely, R. Lau, and C. Gabriel, "The dielectric properties of biological tissues: II. Measurements in the frequency range 10 Hz to 20 GHz," *Phys. Med. Biol.*, vol. 41, no. 11, pp. 2251–2269, 1996.

[13] S. Gabriel, R. W. Lau, and C. Gabriel, "The dielectric properties of biological tissues: III. Parametric models for the dielectric spectrum of tissues," *Phys. Med. Biol.*, vol. 41, no. 11, pp. 2271–2293, 1996.

[14] H. Sato, Y. Li, and Q. Chen, "Measurement of dipole antenna in deionized water," in *Proc. Int. Symp. Antennas Propag. (ISAP)*, Hobart, TAS, Australia, Nov. 2015, pp. 1–3.

[15] A. Saeedfar, H. Sato, and K. Sawaya, "Numerical and experimental impedance analyses of dipole antenna in the vicinity of deionized water at different temperatures," *IEICE Trans. Commun.*, vols. E91-B, no. 3, pp. 963–967, 2008.

[16] Y. Li, H. Sato, and Q. Chen, "Design of capsule dipole antenna for ingestible endoscope," in *Proc. IEICE Tech. Committee Antennas Propag. (AP)*, Feb. 2016.

[17] G. Gonzalez, *Microwave Transistor Amplifiers: Analysis and Design*. Upper Saddle River, NJ, USA: Prentice-Hall, 1996, pp. 84–97.

[18] Q. Chen, K. Ozawa, Q. Yuan, and K. Sawaya, "Antenna characterization for wireless power-transmission system using near-field coupling," *IEEE Antennas Propag. Mag.*, vol. 54, no. 4, pp. 108–116, Aug. 2012.

[19] H. Sato, Y. Li, and Q. Chen, "Experimental study of transmission factor through conducting human body equivalent liquid," in *Proc. Int. Symp. Antennas Propag. (ISAP)*, Oct. 2016, pp. 90–991.

[20] Y. Li, H. Sato, and Q. Chen, "Experiment study of transmission characteristics through conducting human body equivalent liquid," *IEICE Commun. Express*, vol. 6, no. 6, pp. 286–291, Jun. 2017.

[21] Y. Li, H. Sato, and Q. Chen, "Capsule antenna design based on transmission factor through the human body," *IEICE Trans. Commun.*, vol. E101-B, no. 2, pp. 357–363, Feb. 2018.

[22] Y. Li, H. Sato, and Q. Chen, "Study on propagation loss through human body for wireless capsule application," in *Proc. Int. Symp. Antennas Propag. (ISAP)*, Phuket, Thailand, Oct./Nov. 2017, pp. 1–2.

[23] H. Sato, Y. Li, J. Xu, and Q. Chen, "Design of inner-layer capsule dipole antenna for ingestible endoscope," in *Proc. Int. Symp. Antennas Propag. (ISAP)*, Busan, South Korea, Oct. 2018, pp. 1–2.

**YANG LI** received the B.E. and M.E. degrees from the College of Information Technology and Science, Nankai University, Tianjin, in 2008 and 2012, respectively, and the Ph.D. degree from the Department of Engineering, Tohoku University, Sendai, in 2017. He is currently with the College of Electronic and Communication Engineering, Tianjin Normal University. His research interests include antenna design, EM-wave propagation, and sensor networks.

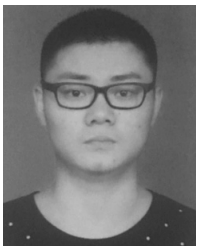

**LICHENG YANG** is currently pursuing the bachelor's degree with the College of Electronic and Communication Engineering, Tianjin Normal University, Tianjin, China.

His current research interests include wireless communication, EM-wave propagation, and sensor networks. He is participating in the Excellent Students' Training Project and the Future Engineer's Training Project.

**WENQING DUAN** is currently pursuing the bachelor's degree with the College of Electronic and Communication Engineering, Tianjin Normal University, Tianjin, China.

Her current research interests include wireless communication, EM-wave propagation, and sensor networks. She is participating in the Excellent Students' Training Project and the Future Engineer's Training Project.

**XIAONAN ZHAO** received the Ph.D. degree from Tianjin University, Tianjin, in 2015. He is currently with the College of Electronic and Communication Engineering, Tianjin Normal University. His research interest includes wireless communication channel measurement and modeling.